Advanced Journal of Chemistry-Section A, 2019, 2(4), 347-364

http://ajchem-a.com

Research Article

Adsorption of Cd (II) and Pb (II) Using Physically Pretreated Camel Bone Biochar

Mohamed Nageeb Rashed*, Allia Abd-Elmenaim Gad, Nada Magdy Fathy

Faculty of Science, Aswan University, 81528 Aswan, Egypt

ARTICLE INFO

Received: 15 April 2019
Revised: 06 May 2019
Accepted: 05 June
Available online: 10 June

DOI: 10.33945/SAMI/AJCA.2019.4.8

KEYWORDS

Wastewater
Lead
Cadmium
Camel Bone
Biochar

ABSTRACT

In this study, low-cost biochar adsorbent originated from camel bone was prepared by physical treatment, and the prepared camel bone biochar for the removal of Cd^{2+} and Pb^{2+} from aqueous solutions was examined. The characterization of the prepared biochar adsorbent before and after the treatment with the metal solutions was done by using XRD, SEM, FT-IR, and BET surface isotherm. The bone sample was pyrolyzed at temperature 500, 600, 800, and 900 °C. Adsorption efficiency of Pb and Cd were optimized by varying different parameters viz., pH, pH_z, contact time, initial metal concentration, adsorbent dosage, and temperature. Nature of the adsorption process is predicted by using adsorption kinetic, isotherms, and thermodynamic models. The results revealed that the effective pyrolysis of camel bone achieved at 800 °C which possess high removal capacity. The maximum adsorption removal percentage for Cd and Pb were 99.4 and 99.89%, respectively at contact time of 1 h, adsorbent dosage of 1 g, pH=5, and initial metal concentration 10 mg/L of both metal salts. The kinetic results of cadmium and lead adsorption obeyed a pseudo-second-order model and fitted well with the Langmuir isotherm.

GRAPHICAL ABSTRACT

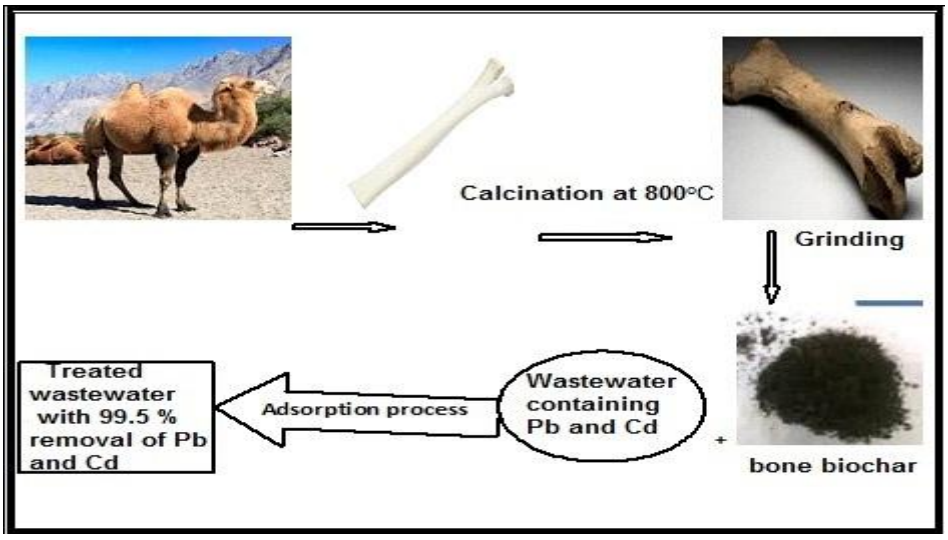

* Corresponding author's E-mail address: *mnrashed@hotmail.com*

Introduction

Aquatic pollution by heavy metals is a great problem. The presence of heavy metals in the aquatic environment is the most problem effects the health of humanity, as it is non-degradability and, so it's toxic in water [1]. The existence of low levels of the heavy metals in water resources will accumulate in the food chain and lead to its contamination with toxic heavy metals [2].

Several techniques are available for the treatment of heavy metals pollution from polluted water *viz*., catalysis, ion exchange, reverse osmosis, precipitation adsorption, and coagulation. Among these technologies, adsorption has a wide application. The adsorption of heavy metal depends on the nature of the adsorbents which prepared from several sources which include natural resources, including tree ferns and composites [3], plants, industrial waste, clays, activated carbon, sludges, algae, wheat bran, shells [4], agricultural wastes and cork Yohimbe bark wastes [5], tire rubber [6-7].

Bone char is an adsorbent consisting of 90% calcium phosphate and 10% carbon and is produced by two main treatments which include chemical treatment by several chemicals, and physical treatment by carbonization of bones. The structure of bone char is calcium phosphate in the hydroxyapatite form ($Ca_{10}(PO_4)_6(OH)_2$, HAp) which is known for its more effective adsorption properties which can adsorb divalent heavy metals [8].

Camel bone char was applied widely for the treatment of polluted water with heavy metals. Alqadami *et al.* [9] prepared magnetic nanocomposite from camel bones and used it for adsorption of toxic metals from water. Hassan *et al.* [10] prepared camel bone charcoal and applied it for the removal of mercury ions from wastewater. Ramavandi *et al.* [11] reported the efficiency of camel bone powder for the removal of copper from wastewater.

The aim of this study is to prepare low cost, effective and eco-friendly camel biochar adsorbent from camel bone by physical activation (carbonization) and applying the developed adsorbent for the removal of two heavy metals (Pb and Cd) from the polluted water.

Experimental

Reagents and standards

The reagents and chemicals used were of analytical grade (Merk and BDH). Deionized water was used throughout the study to carry out all the experiments. Metal (Cd and Pb) standard solutions were prepared by using analytical grade samples [$Pb(NO_3)_2$, $Cd(NO_3)_2$]. pH was adjusted to the suitable values for each experiment by pH meter using solutions of HNO_3 or NaOH.

Camel bone collection and pretreatment

Discarded Camel bones were purchased from local butchers shops. In order to remove the fat and flesh from the Camel's bone, it is washed with hot deionized water several times; then the bones were left to dry in the open air. The air-dried bones are oven dried in an oven at 110 °C overnight. The dried bones were crushed, sieved to particle size (<63 μm) and stored in dry containers which may be used to carry out the experiments.

Biochar adsorbent preparation

The dried bone was calcinated at 500 °C up to 900 °C by varying time (1, 2 and 3 h) in a muffle furnace with a limited supply of oxygen. The resulted biochar bone adsorbents were grounded with agate mortar, sieved to particle size (<63 μm) and stabilized to the further experiments.

Adsorbate preparation

1000 mg/L Pb and Cd stock standard solutions are prepared by using deionized water. The working metal ions solution was prepared from the stock solution by dilution.

Batch adsorption experiments

Batch adsorption experiments performed such as Z_{pHc}, pH, initial metal ions concentration, adsorbent dosage, temperature and contact time.

The effect of camel biochar dose on the adsorption of the metal was studied by carrying out using different masses of the camel biochar in a range between 0.01 and 1 g. The effect of contact time on the adsorption of Cd and Pb onto camel biochar were verified with 30, 60, 120, and 180 minutes. For the effect of initial metal concentration on adsorption, the metal ions (Cd and Pb) concentration were varied from 10 to 70 mg/L. For studying the effect of pH, the values of pH were in a range from 3 up to 9. The final and initial pH values in the Z_{pHc} were measured in which a 50 mL solution of 0.1 M NaCl was in contact with 0.1 of camel biochar bone. From plotting initial pH and final pH, the point of the intersection gave the Z_{pHc} [12].

Analytical measurement of heavy metals

Heavy metal concentrations in the filtrate were determined after each experiment by atomic absorption spectrometer (AAS) [THERMO SCIENTIFIC Ice 3000].

The adsorption capacities of Cd^{2+} and Pb^{2+} were calculated by the following equation:

$$q=V\ (Ci- Ce)/W$$

Where q is adsorption capacity (mg/g), C_e metal concentration at equilibrium (mg/L), C_i initial metal concentration (mg/L), W camel biochar adsorbent dosage (g) and V solution volume (L).

Removal percentage of the heavy metal ions were calculated:

$$\text{Removal } \% = \frac{\text{Ci}-\text{Ce}}{\text{Ci}} \times 100$$

Characterization of Camel bone biochar adsorbent

X-ray diffraction (XRD) spectra of camel bone and the prepared camel biochar adsorbents were characterized using a Bruker D8 Advance diffraction system, with Cu Ka radiation in theta/theta reflection geometry. The surface morphology of the prepared camel biochar adsorbents was investigated by scanning electron microscope (SEM, JEOL_ JSM-6400). FTIR spectra of both original and prepared adsorbents were performed by Bomem MB100 FTIR spectrometer recorded in the 4000–400 cm^{-1} region. The specific surface area and pore size distributions of the adsorbent were determined by applying the adsorption-desorption BET method using nitrogen as an adsorbate, at 77 K.

Results and discussion

Characterization of Camel bone biochar

XRD

X-ray diffraction (XRD) patterns (Figure 1 a, b) show morphology of the camel bones before and after calcination from the Figures, it was noticed that the camel bones sample displays the same characteristic peaks as standard hydroxyapatite, where it shows three intense peaks at 31.8°, 32.22° and 33.01° corresponding to Miller indices (211), (112) and (300) respectively, less intense peaks at 2θ of 25.9°, 39.8°, 46.73°and at 2θ=49.48°-53.24° also at 2θ=28.13°-29.02°. X-ray diffraction spectra of the adsorbents (camel biochar) show the crystalline structure of hexagonal calcium

hydroxyapatite ($Ca_{10}(PO_4)_6(OH)_2$ or calcium phosphate hydroxide (Figure 1 b) While the camel bone before activation shows the approximately amorphous phase of hydroxyapatite with very low-intensity peaks as shown in (Figure 1 a).

FTIR

The FTIR study of the camel bone biochar provided us with information about the mechanism of adsorption. FTIR spectrum of the camel bone biochar before calcination (CB) (Figure 2 a) indicates presence of hydrocarbon groups peaks of -CH stretching at 2853-2923 cm^{-1}, the large peak located at 3000-3600 cm^{-1} assigned to the crystallization water (OH groups), the absorption bands due to C=N, C=O, C=C stretching modes were observed at (1465-1744 cm^{-1}).

A broad and strong band attributed to phosphate ($PO4^{3-}$) group were noticed at (1100-900 cm^{-1}) and the absorption bands at 720 cm^{-1} suggest the presence of CO_3^{2-} in hydroxyapatite structure. Moreover, a broad and strong band of calcium of Ca^{2+} was observed at (550-610 cm^{-1}) that indicated the structure of calcium hydroxyapatite. After carbonization (CB800) (Figure 2 b), no peaks were noticed due to protein and collagen (C=N, C=O, C=C), while the peaks due to OH group (3000-3600 cm^{-1}) and hydrocarbon of -CH stretching (2853-2923 cm^{-1}) were reduced after calcination. However, the main functional groups, phosphate and calcium peaks remain unchanged. Elliot [13] reported in bone IR spectrum strong split phosphate (PO_4^{3-}) bands in the range 1, 100–1, 000 cm^{-1} (stretching mode) and 500–600 cm^{-1}. These bands are characteristics of mineral phases of teeth and bone, calcium hydroxyapatite [$Ca_5(PO_4)_3(OH)$].

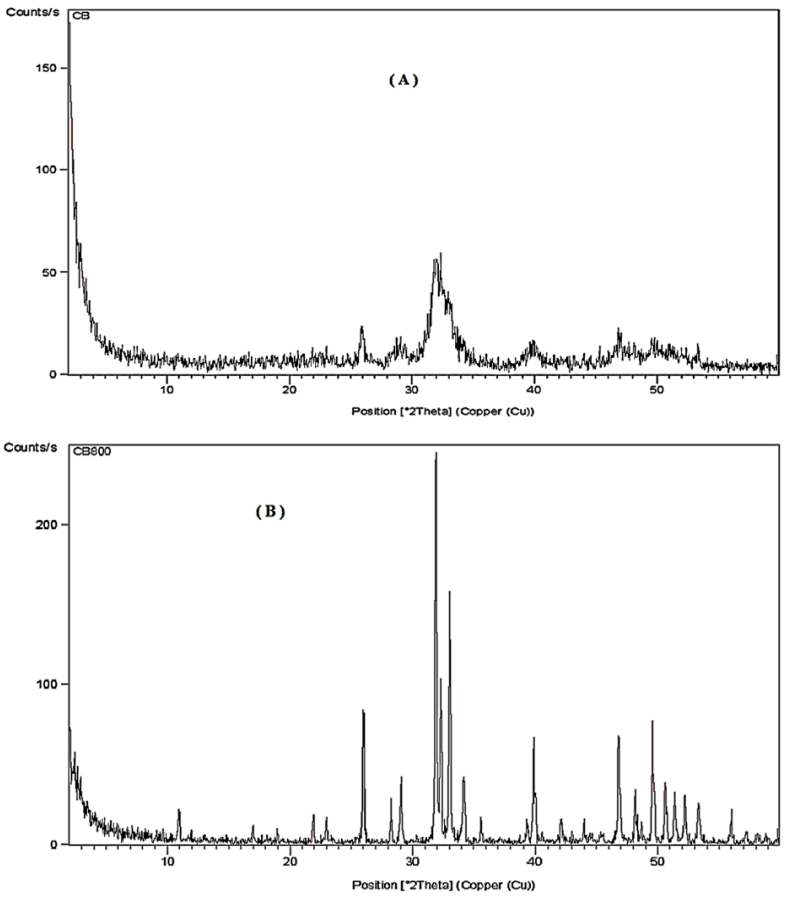

Figure 1. XRD of camel bone before (A), and after calcination (B)

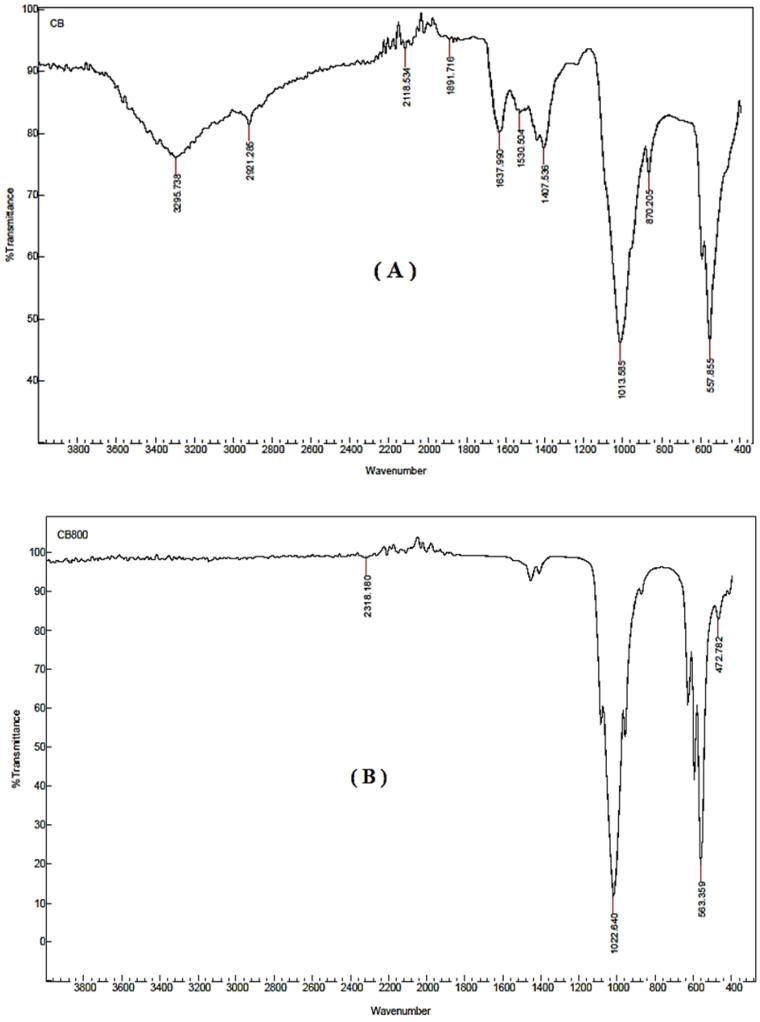

Figure 2. FTIR of camel bone before calcination (A), and after calcination (B)

SEM

The SEM micrographs of the camel bone biochar explained the morphology of the adsorbents before and after calcination by analyzing the microstructure bones powder (Figure 3). The untreated camel bone powder particles show a cluster with various sizes, very irregular shapes and present a texture varying from rough to smooth surface. The surface of the samples after calcination have become rough with an undefined geometry and the morphology.

The graphs (Figure 1) show that there was a cracked and irregular surface in the adsorbents. The minimum particle size before calcination (the raw material) was 5.529, 7.772 and 9.922 µm and after calcination at 800 °C for 2 h. It is obvious that the surface morphology changes and the particle size decreased to 3.503, 2.627 and 4.147 µm. Furthermore, it was noticed that the samples have several numbers of heterogeneous porous layer and pores which may be playing a significant role in the absorption of heavy metals [14].

BET (Brunauer, Emmett and Teller)

The surface area is very effective property described the adsorbent surface nature, and so it can be clearly distinguished between camel bone sample before and after treatments. The BET method is the most common method for measuring the surface area of adsorbents using nitrogen gas as adsorbate onto the

surface of the material. The results reveal that the measuring surface area of the camel bone before calcination was 14.55 m^2/g, while after calcination it was raised to 74.8 m^2/g, which indicates that the surface area of the camel bone increase after calcination. This result was in a good agreement with XRD, and SEM analysis as the hydroxyapatite peaks became more crystalline, and the particle size reduces after calculation.

Effect of pyrolysis temperature on adsorbent efficiency for the removal of heavy metals

The data From (Table 1) reveals that the optimum calcination temperature for the high removal of cadmium (99.4%) and lead (99.89%) was at 800 °C with a calcination period two hours.

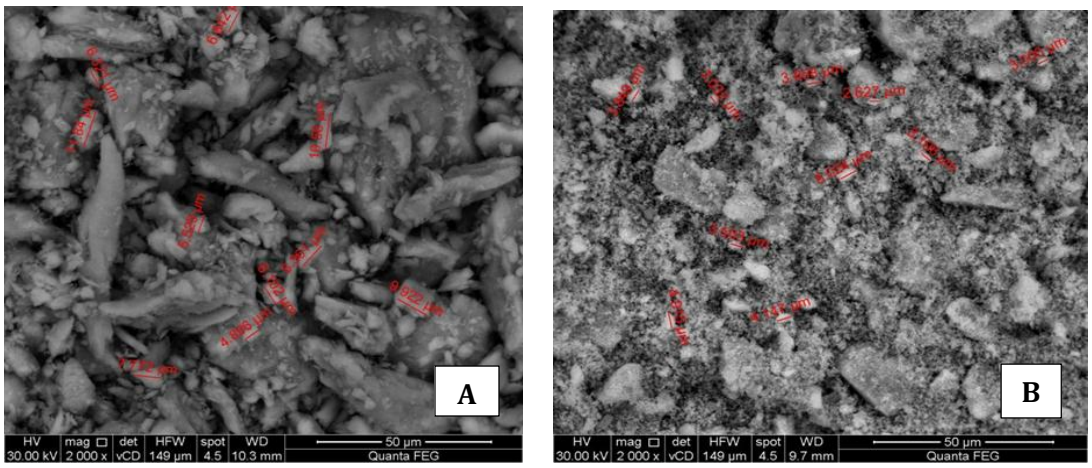

Figure 3. SEM of camel bone before calcination (A), and after calcination (B)

Table 1. Removal percentage of Cd and Pb ions after the calculation process

Temp (°C)	Cd% Time			Pb% Time		
	1h	2h	3h	1h	2h	3h
500	99.0	99.2	96.9	99.04	99.21	99.2
600	99.1	98.6	98.4	99.16	99.69	99.68
800	98.2	99.4	87.3	99.3	99.89	99.71
900	93.9	88.2	83.2	99.78	99.62	99.53

The increase in calcination temperature and time the surface area increase due to a reduction in particle size. On the other hand, at a high temperature, an aggregation of the particles occurs which resulting in less removal efficiency. So the camel adsorbent was prepared at this 800 °C calcination temperature and labeled as CB800.

Optimal conditions for metal adsorption

Effect of the initial adsorbent dose

From Figure 4, it is observed that as the adsorbent dose increased up to 1 g, the removal efficiency of the metal increased

up to 99.8% for lead and cadmium. This increase was as the result of increasing the adsorption sites on camel bone adsorbent. After adsorbent dose (1 g) by increasing the adsorbent dose the metal removal decreases as a result of a competition between the empty sites on the adsorbent surface to attract the metal ions [15-16].

Effect of initial pH

The efficiency of metal removal and nature of camel bone biochar surface depends mainly on the pH value of the solution. From Figure 6 it was observed the removal of Pb and Cd ions increase with the increase in pH value, and reaching the maximum adsorption of Cd and Pb at pH=5. This was explained that at the low pH values, hydrogen ions increase on the adsorbent surface which led to less attraction to metal ions, while at high pH values the adsorbent biochar surface became negatively charged and attract metal ions. Other studies reveal that the adsorption of cadmium was pH dependent and the maximum removal was obtained at two different pHs (pH 5.0 and 8.0) [17].

Determination of pH at the point of zero charge (pH_{PZC})

The methodology for determining the point of zero charge (pH_{PZC}) was adapted from that described by". PH_{pzc} is known as an "eleven point PZC" and defined as the pH at which the charge on the surface of solid equal zero [12]. This study was carried out with 0.025 g of camel bone biochar adsorbent and 10 mL 0.1 N NaCl solution at varied of initial pH (2-12) and agitated on a shaker at 250 rpm at 25 °C for 1 h. The initial pH versus the final pH was plotted (Figure 6), and the range where the pH of the solution remains constant is taken as the pH at the point of zero charge (pH_{PZC}) [18]. The results showed that the zero point charge matched with the study of pH (pH=5). Since the solution pH is acidic, the surface charge of the camel bone biochar is positive owing to the existence of neutral and positively charged ($=POH^{o}$ and $=CaOH_2^{+}$) sites which cause the positive camel bone biochar surface [19]. The adsorption of metal cations is favored at $pH>pH_{PZC}$, while the adsorption of anions is favored at $pH < pH_{PZC}$, due to electrostatic attraction [20-21].

In a study of lead ion adsorption onto activated carbon adsorbent originating from cow bone [22], they reported that the pH_{PZC} was 4.0 as a result that at the adsorbent surface higher amount of acid functional groups were presented than basic groups, making it easy for cationic exchange

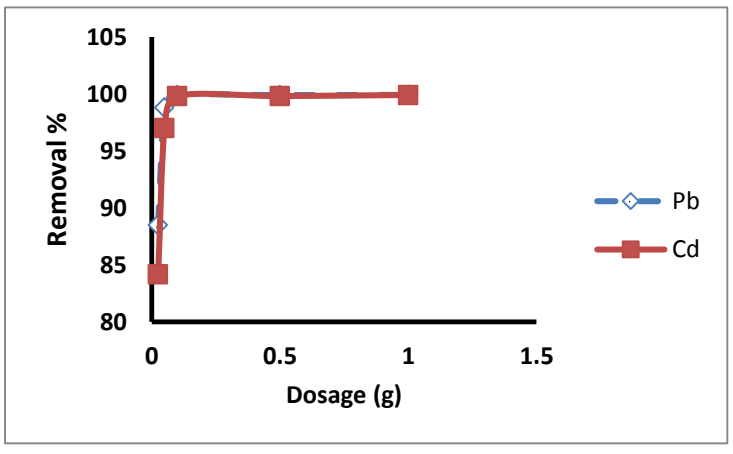

Figure 4. The relation between the adsorbent dosage and the metal ions removal

Figure 5. The effect of pH on the removal percentage of lead and cadmium ions

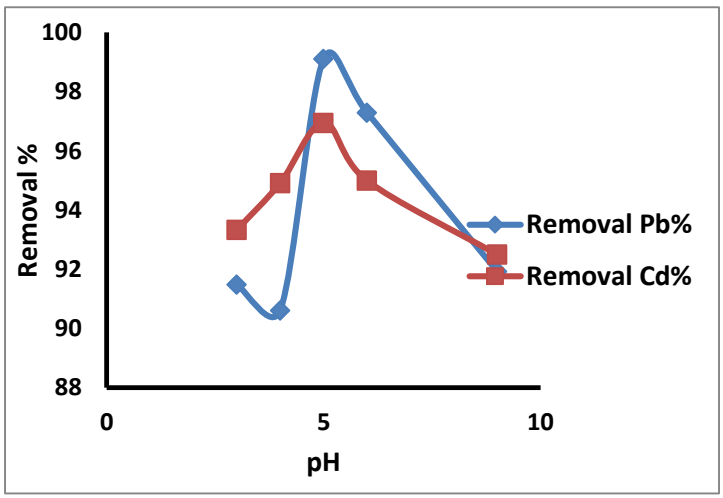

Figure 6. Curve of pH at point of zero charge (pH_{PCZ})

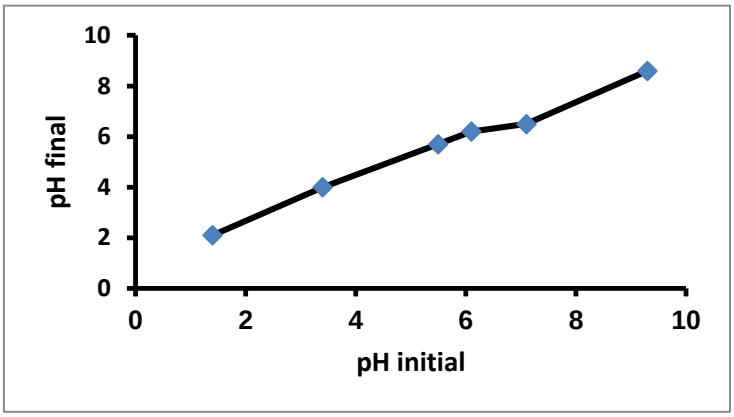

Effect of initial metal ions concentration

The metal uptake depends on the active sites as well as on the nature of the metal ions in the solutions. The results (Table 2) show that 10 mg/L metal concentration was the best metal ions concentration for high removal of Cd and Pb, while the affinity of adsorbent towards Pb ions was more than Cd ions, and this may be associated with the size of the ion and the porosity of the camel bone biochar. At a low metal ions concentration 10 mg/L, the adsorbent surface sites were active and had an affinity to be occupied by a metal ion, while at higher metal ions concentration, the active sites were filled with the ions which cause the metal ions remained in the solution owing to saturation of active sites of adsorbent.

Effect of contact time

From Figure 7, it was obvious that the adsorption efficiency of Pb and Cd increased rapidly and reached the maximum at 60 minutes after then there wasn't any additional removal of Pb and Cd ions; because of the complete occupied sites on the surface of the adsorbent.

Adsorption kinetic

The first-order rate equation (Lagergren), the second-order rate equation were used as kinetic models in the description of the adsorption process

between adsorbent and adsorbate.

The pseudo first order

The first-order rate equation is:

$$\text{Log } (q_e\text{-}q_t)=\log q_e - (K_1/2.303).t$$

Where q_e is the amount of the metal ions adsorbed on the adsorbent, and q_t (mg/g^{-1}) is that at equilibrium time (t), t (min) is the contact time, and K_1 (min^{-1}) is the rate constant of the first-order adsorption model.

By the plot of log (q_e-q_t) versus t, the intercept and the slope could be obtained from. Data obtained from the pseudo-first is summarized in Table 3. The results reveal a higher correlation coefficient R^2 for Pb (0.965) than that for Cd (0.6403).

The pseudo Second-order model

The pseudo Second order equation is

$$\left(\frac{t}{qt}\right) = \left(\frac{1}{k_2 q_e^2}\right) + \left(\frac{t}{q_e}\right)$$

where qe, q_t (mg g^{-1}) is the amount of the metal ions adsorbed at equilibrium and at the time (t) respectively, K_2 is the pseudo-second-order constant (g mg^{-1}/min $^{-1}$).

A plot of t/q_t vs t shows a linear relationship with correlation coefficient (R^2). k_2 and equilibrium adsorption capacity q_e were calculated from intercept and slope of the plot. Data obtained from the pseudo-second is summarized in Table 3.

Table 2. Effect of initial metal concentration on the adsorption efficiency of camel biochare

Metal concentration ppm	Equilibrium Pb concentration(Ce) ppm	Removal% Pb	Equilibrium Cd concentration(Ce) ppm	Removal % Cd
10	0.03	99.7	0.065	99.35
20	0.075	99.62	0.1769	99.11
40	0.139	99.65	5.4073	86.48
60	0.221	99.63	10.849	81.92
70	0.295	99.58	35.109	49.84

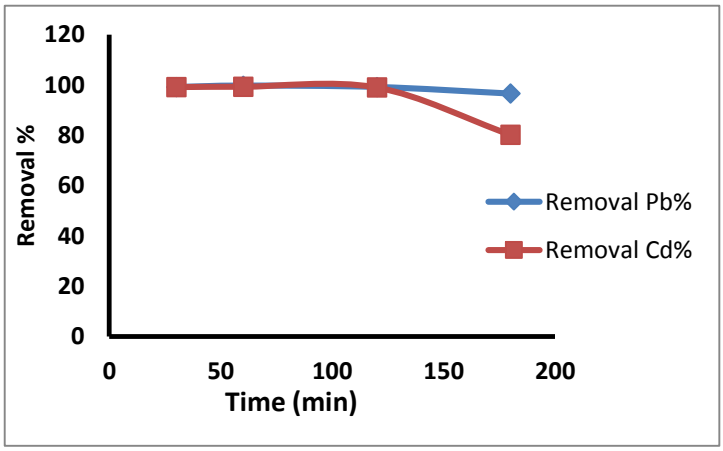

Figure 7. Effect of contact time on the removal of cadmium and lead solution at 25^{o}C

The correlation coefficient (R^2) for pseudo-second order is higher than that for the pseudo-first-order so that the adsorption of Pb and Cd by camel biochar adsorbent followed the pseudo-second order kinetic.

The experimental q_{ex} and calculated q_e values are very close, indicating the applicability of pseudo-second-order to describe the adsorption of Pb and Cd on camel biochar described by the pseudo second-order model only.

Ho and Mc Kay [23] reported that most of the sorption systems followed a second-order kinetic model.

Intra-particle diffusion model

There are two types of diffusion, Boundary and intra-particle diffusion. Boundary layer diffusion is described by the initial rate of the metal ions adsorption [19].

The solute transfer could be characterized by intraparticle diffusion model which explain the mechanism of the of solid-liquid adsorption [24] as the following:

$$q_t = K_i\, t^{½} + C$$

Where, q_t is the adsorbed amount at time t, K_i (mg g^{-1} $min^{-1/2}$) is the rate constant of the intra-particle diffusion model, C (mg g^{-1}) is the boundary layer effect.

From the linear plot of q_t vs $t^{1/2}$ (Fig.8), the values of C and K_i can be obtained from the intercept and slope (Table 3).

From Figure 8 it is obvious that there are linear and plateau sections. The linear section refers to the intra-particle diffusion, while the plateau one refers to the equilibrium. This indicates that the transport of Pb and Cd ions from solution to the adsorbent through the particle interface into the pores of the adsorbent.

k_{id} associated with the adsorption rate in the intraparticle diffusion. The extrapolation of the linear curve parts of the plots back to the axis provides the intercepts, which are proportional to the extent of the boundary layer thickness, *i.e.,* the larger the intercept, the greater the boundary layer effect. The deviation of the curves from the origin indicates that intra-particle transport is not the only rate limiting step [25].

Table 3. Kinetics constants of pseudo-first-order, pseudo-second order and intra particle diffusion for adsorption of Pb and Cd ions on the Camel biochar adsorbent

Parameters	Pb	Cd
	Pseudo first-order	
K_f $(min)^{-1}$	-0.0011	-0.02
R^2	0.966	0.640
	Pseudo second-order	
K_2 (g/mg min)	0.28	0.53
q_e (mg/g)	1.924	1.62
R^2	0.999	0.981
q_{ex}	1.994	1.987
	Intra particle diffusion model	
K_{id}	0.0017	0.0012
C (mg g^{-1})	1.977	1.975
R^2	0.792	0.942

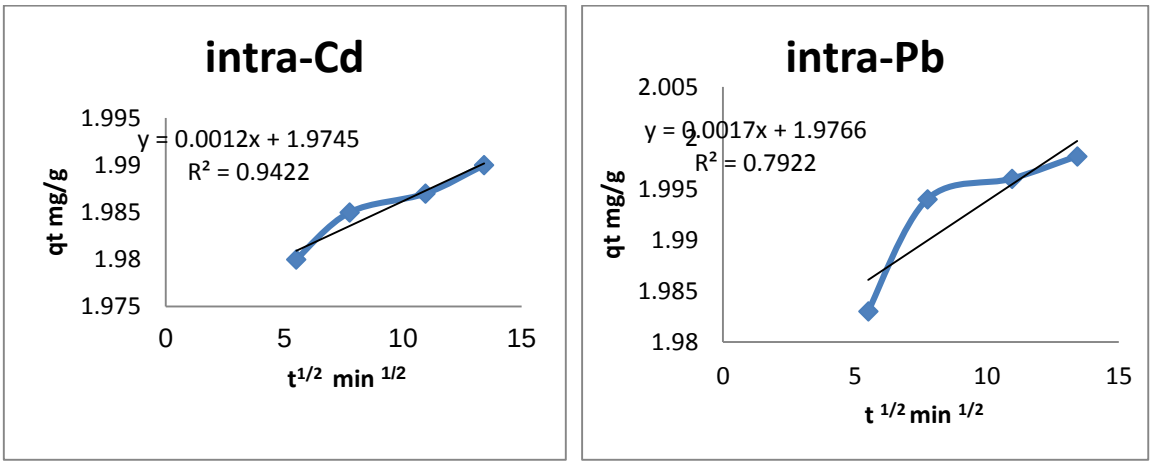

Figure 8. Intra-particle diffusion model of cadmium and lead ions

Adsorption isotherm models

For an adsorption isotherm experiment, 0.10 g of camel bone biochar was shaken with 20 mL of metal ions (Pb and Cd) solution in concentrations ranging from 10 to 70 mg/L at 25 °C± 0.3 and pH=5.

The resulted mixture was then filtered, and the filtrate was analyzed by AAS for Pb and Cd concentrations. The amount of metal ions adsorbed at equilibrium was calculated in (mg g^{-1}) from this equation:

$$q_e = \frac{(C_0 - C_e).V}{m}$$

Where; q_e is the amount of adsorbed metal ions at equilibrium (mg/g^{-1}), C_o is the initial metal ions concentration (mg/L^{-1}), C_e the concentration of metal ions at equilibrium (mg L^{-1}), V is the volume of metal ions solution (L), m is the mass of adsorbent (gm).

Linear isotherm model

The linear model describes the adsorption of solute by sorbent as follows:

$$q_e = K_d .Ce$$

Where q_e, is the amount of adsorbate (mg/g), K_d equilibrium distribution coefficient, Ce equilibrium concentration of the metal.

The linear isotherm is a special case of the Freundlich isotherm where the Freundlich exponent (n) is equal to 1.

By plotting of q_e versus Ce a linear line was obtained (Fig.9), and K_d was calculated which was 50.8 for Pb and 0.984 for Cd. These results indicated that the equilibrium distribution K_d of Pb ions on the surface of the adsorbent was higher than that for Cd ions.

Langmuir isotherm model

Langmuir equation explained the homogenous nature of the surface of the adsorbent. This equation is favorable in descriptive and qualitative purposes rather than a quantitative one.

The equation is:

$$\left(\frac{Ce}{qe}\right) = \left(\frac{1}{Q_0 b}\right) + \left(\frac{Ce}{Q_o}\right)$$

Where C_e (mg/L^{-1}) is the concentration of metal ions at equilibrium, Q_o (mg/g^{-1}) is the maximum amount of metal ions per unit weight adsorbent, q_e (mg/g^{-1}) is the amount of adsorbed metal ions at equilibrium, b (L/mg^{-1}) is binding energy constant. By plotting $\left(\frac{Ce}{qe}\right)$ *vs Ce* , Langmuir constants were obtained (Figure 10, Table

4).
R_L value was calculated from the obtained b and Q_o values, according to this equation:

$$RL = \frac{1}{1 + b\ Qo}$$

R_L refers to the separation factor. Since, R_L>1, the isotherm is unfavorable model, R_L=1 refers to be a linear isotherm, 0<R_L<1 the isotherm is favorable for the study; and R_L = 0 the isotherm is irreversible type.

So, from the results, R_L values obtained were 0.015 and 0.067 for Pb^{2+} and Cd^{2+}, respectively, and so that these values were between 0 and 1, showing that the model is favorable to this study.

Freundlich isotherm model

Freundlich isotherm model applied for multi-layer adsorption on a heterogeneous adsorbent surface with sites that have different energies of adsorption. Freundlich equation is:

$$\log q_e = \log K_f + \frac{1}{n} \log C_e$$

Where qe (mg/g^{-1}) is the amount of adsorbed metal ions at equilibrium, K_f is

Table 4. Results of isotherm plot parameters for adsorption of Cd and Pb ions onto Camel biochar adsorbent

Parameters	Cd	Pb
Linear adsorption model		
K	0.32	50.8
R^2	0.421	0.974
Langmuir sotherm model		
Q_0	7.02	57.8
b_L (L/mg)	1.99	1.11
R^2	0.99	0.986
Freundlish isotherm model		
1/n	0.213	0.885
K_f ($mg^{-1/n}$ $L^{1/n}$ g^{-1})	4.65	43.25
R^2	0.804	0.886
Temkin isotherm model		
B (j/mol)	0.0197	5.37
b_T	125,765	461.6
Kt (L/g)	1494.6	38.3
R^2	0.7597	0.9363
Dubin-Raduskevich isotherm model		
q_D (mg/g)	7.8	20.9
E (kj/mol)	4.1	4.0
β (mol^2/kJ^2)	$3*10^{-8}$	$3*10^{-8}$
R^2	0.956	0.963

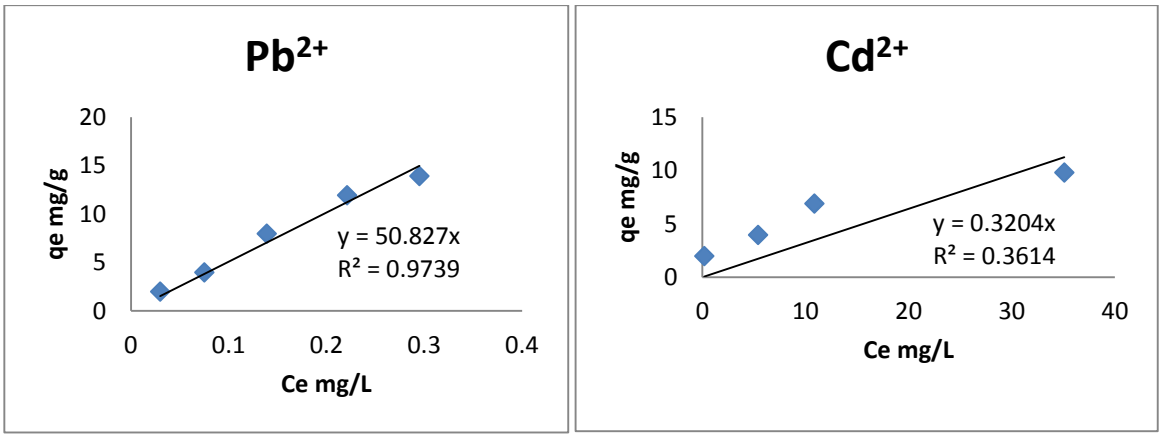

Figure 9. The adsorption linear model of cadmium and lead ions

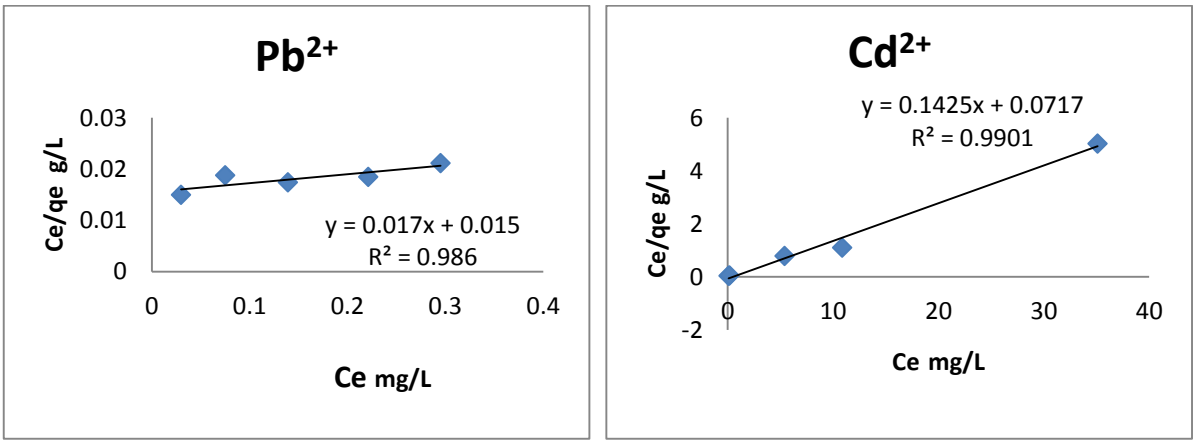

Figure 10. The Langmuir model of cadmium and lead ions

Freundlich constant related to the adsorption capacity, 1/n is Freundlich constant related to adsorption intensity of the adsorbent.

By plotting $\log q_e$ versus $\log C_e$ (Figure 11, Table 4) a linear plot was obtained, then the values of k_f and l/n were evaluated from the intercept and the slope. The results revealed that the 1/n values are less than 1, which indicate that the Pb and Cd ions are favorably adsorbed by camel bone biochar.

Concerning the Langmuir and Freundlich values, Langmuir isotherm showed a greater match than Freundlich for Pb and Cd; because the correlation coefficient (R^2) provides an optimum fit to the obtained data.

So, Langmuir adsorption isotherm shows an appropriate description of Pb and Cd adsorption than Freundlich isotherm.

Temkin isotherm model

Temkin isotherm model is used for expressing the uniform distribution of binding energies over the population of surface binding adsorption. The linear form of Temkin equation is expressed as:

$$q_e = B \ln K + B \ln C_e$$

$$B = RT/b$$

Where, qe (mg/g) is the amount of adsorbed metals per unit weight of camel bone adsorbent, Ce (mg/L) metal ions concentration in solution at equilibrium, b is the Temkin constant related to the heat

of sorption (J/mol).

By drawing a plot between qe versus $\ln C_e$ (Figure 12), the constant B (J/mol) and K (L/g) were obtained and listed in (Table 4). From Table 4, it found that the B and K values of Pb^{2+} were lower than that for Cd^{2+} so that Pb^{2+} have a larger heat of adsorption than Cd^{2+}.

Dubinin-Radushkevich isotherm model (D-R model)

Dubinin-Radushkevich isotherm is used to describe the adsorption with a Gaussian energy distribution onto a heterogeneous surface, and so it is described to compare between physical and chemical adsorption of the metal ion.

The linear form of the D-R equation is:

$$\text{Ln qe} = \ln q_m - \beta E^2$$

Where q_m is a constant that indicates the sorption degree characterizing the adsorbent (mg/g), β is a constant related to the adsorption energy (mol^2/kJ^2), and E is the Polanyi potential, which can be calculated by the following equation:

$$E = RT \ln (1+1/C_e)$$

Where R, is the ideal gas constant and T is absolute temperature (K).

By drawing a curve between lnqe vs. E^2 (Figure 13, Table 4), the value of qm and β can be obtained from the slope and the intercept, respectively.

The mean free energy E (KJ/mol) of sorption can be estimated by using B values from the following equation:

$$E = \frac{1}{\sqrt{2\beta}}$$

The value of E may characterize the type of the adsorption as chemical ion exchange (E=8-16 kJ/mol), or physical adsorption (E<8 kJ/mol) [26]. From the E values of Cd^{2+} (4.1) and Pb^{2+} (4.0), it is obvious that the adsorption is considered as physical adsorption.

Thermodynamic adsorption study

The thermodynamic parameters, Gibbs free energy (ΔG^o), enthalpy (ΔH^o) and entropy (ΔS^o), are indicators for practical applications.

Adsorption thermodynamics were evaluated concerning different temperatures (298, 313, 323 and 343 K).

The following equation is used to calculate the thermodynamic parameters:

$$\text{Ln k} = \Delta S^o /R - \Delta H^o /RT$$

Where R is the universal gas constant (8.314 J/mol K), and T is temperature (K).

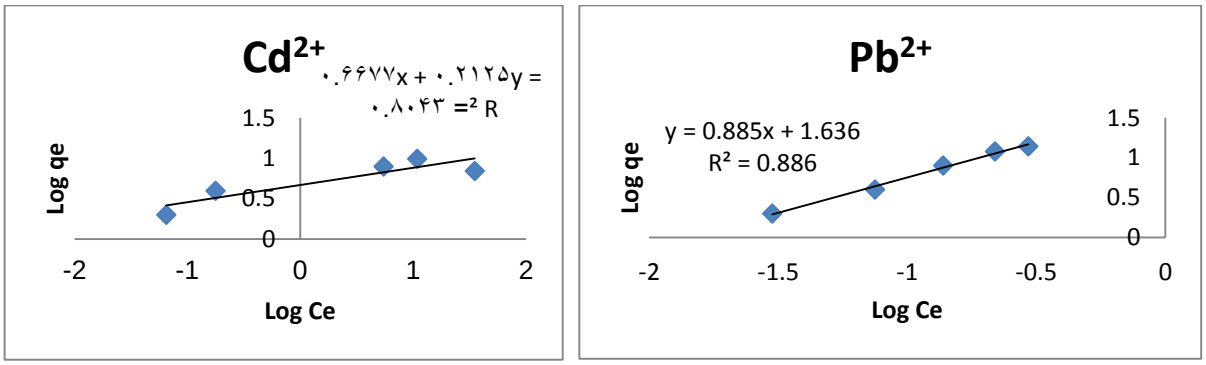

Figure 11. The Freundlish model of cadmium and lead ions

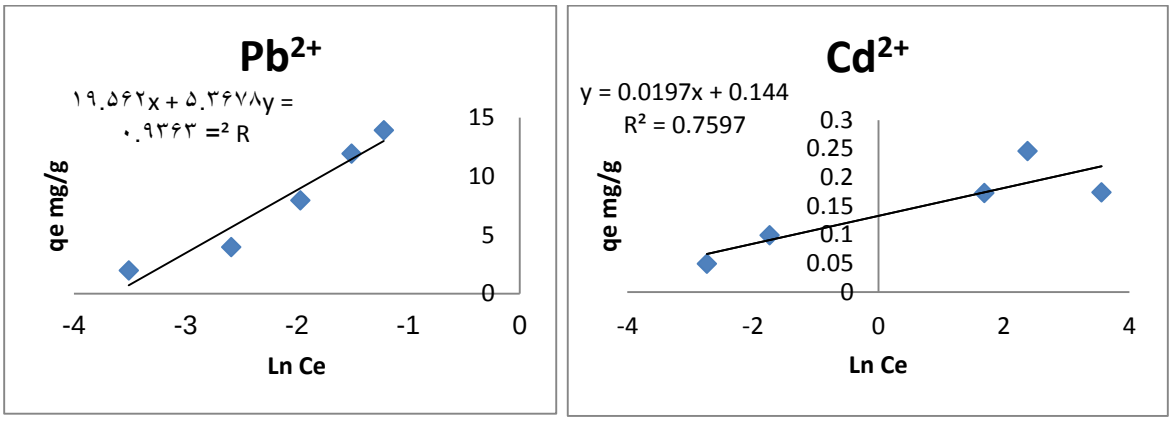

Figure 12. Temkin isotherm model of cadmium and lead ions

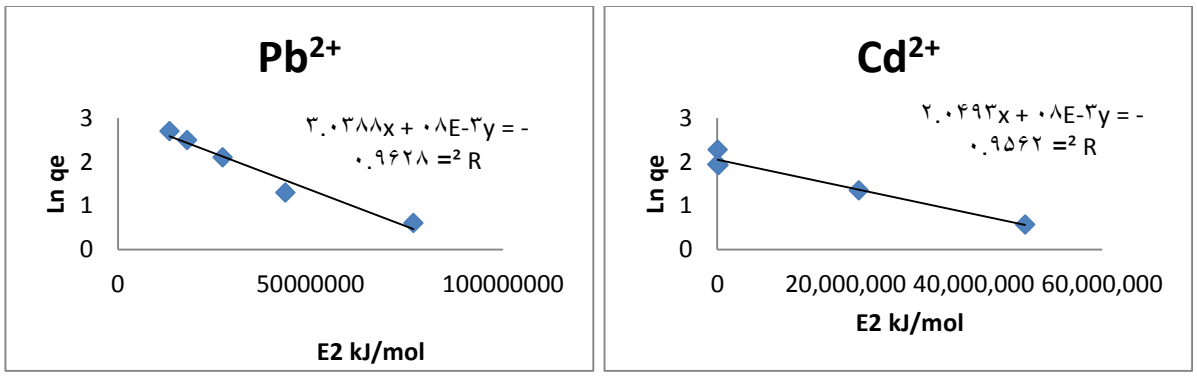

Figure 13. Dubinin-Radushkevich isotherm model of cadmium and lead ions

ΔH^o and ΔS^o were determined from the slope and intercept of the van't Hoff plots of ln k vs. 1/T. The free energy of adsorption (ΔG^0 KJ/mol) is calculated from the following expression:

$$\Delta G^o = \Delta H^o - T\,\Delta S^o$$

$$\Delta Go = -RT\,lnb$$

The resulted thermodynamic parameters are presented in Table (5). From Table 5, the adsorption data of Pb and Cd indicate that $\Delta G°$ values for camel biochar adsorbent were negative at all temperatures, which confirms the spontaneous nature of adsorption of Cd and Pb by camel biochar adsorbent, and that the adsorption is physical adsorption process. The positive values of $\Delta H°$ have confirmed the endothermic nature of Pb and Cd adsorption on camel bone biochar.

Desorption using several desorbed solutions

For desorption experiments, after the adsorption process and separation of liquid phase, the precipitated metal-laden adsorbent was collected after filtration and washed with deionized water several times to remove any adhesive metal ions to the surface of adsorbent, then it was dried in an oven at 60 °C overnight for the next experiments .

For desorption experiment, certain volume of desorbed solutions (0.1N HNO_3, 0.1N NaOH and deionized water) and precipitated metal-laden adsorbent was shaken until reaching the equilibrium, the solutions were separated from the solid phase by centrifuge and the upper layer was analyzed by atomic absorption

spectrometer (AAS) for the metal ions concentration and the desorbed metal ions was calculated by this equation:

$$Desorbed\% = \frac{\text{amount of desorbed ion}}{\text{amount of adsorbed ion (amount taken up during adsorp.)}} \times 100$$

The desorption percentage of 0.1N HNO_3, 0.1N NaOH and deionized water of Pb^{2+} and Cd^{2+} were (93%, 81%, 56%), and (72%, 66%, 59%), respectively (Figure 14). This result ended to that 0.1 N HNO_3 is favorable in the desorption of Pb^{2+} and Cd^{2+} from the metal-laden adsorbent.

Venkata, Rao, & Karthikeyan [27] reported that desorption phenomenon observed in both NaOH and HNO_3 might be attributed to ion exchange type interaction rather than chemical sorption.

Application on real sample

Wastewater sample of the disposal of Kima fertilizer factory at Aswan city was collected and some parameters such as electrical conductivity, pH, TDS, temperature and the concentration of lead and cadmium were measured before the adsorption process. The wastewater sample was filtered. 50 mL of the filtrate was adjusted to pH 5 and shaken with 0.1 g of the camel bone biochar for 60 min at 25 °C, after then it filtered using filter paper. Cd and Pb concentration in the filtrate was measured by atomic absorption spectrophotometer. The results reveal that the removal of lead and cadmium were reached 99.9%.

Table 5. Thermo dynamical parameters for the adsorption of lead and cadmium ions

Parameters		Pb	Cd
ΔH^o, kJ/mol		10.6	5.8
ΔS^o, kJ/ mol K		-0.014	-0.015
ΔG^o, kJ/mol	298 K	- 0.259	- 1.7
	313 k	-0.271	-1.79
	323 k	-0.28	-0.85
	343 k	-0.24	-1.96
R^2		0.4385	0.4519

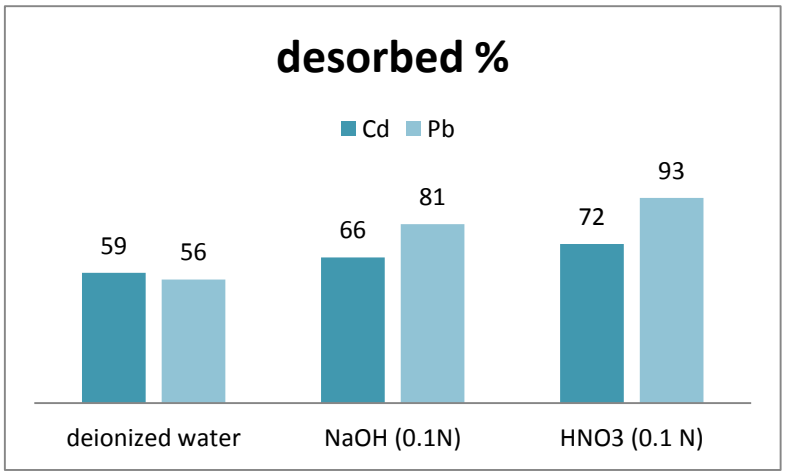

Figure 14. Desorption of cadmium and lead ions using several desorbed solutions

Conclusion

In this study, the primary results indicated that natural camel bone biochar appeared a massive ability of adsorption of pollutants especially heavy metal from the water streams.

The results of batch experimental studies reflected that the adsorption operation depends on pH, contact time, adsorbent dose, initial metal concentration, and solution temperature.

The adsorption equilibrium was gained at 60 min since 99% of metal ions were removed. The adsorption kinetics of lead and cadmium ions followed the pseudo-second-order kinetic model. The linear, Langmuir and Freundlich isotherm models were used to represent the experimental data, and the Langmuir model fitted well the metal adsorption with a Q_o value of 57.8 mg g^{-1} for lead and 7.02 mg g^{-1} for cadmium. The negative value of ΔG^o and ΔS^o showed that the adsorption of the lead and cadmium ions by camel bone biochar was spontaneous. The positive value of ΔH^o confirmed the endothermic nature of adsorption. The simple, clean, and green procedure of this adsorbent would offer a vital technique for industrial wastewater cleanup. So this study reveals the high impact of the animal bones in the removal of the heavy metals from disposal water resources.

Acknowledgment

The authors wish to thank their colleagues at chemistry department, faculty of science, and at the unit of environmental studies, Awan university for their technical help, and also they would like to express their thanks to the chemists at the High Dam Lake Development Authority for their assistance in heavy metals analysis.

ORCID

Mohamed N. Rashed : 0000-0003-2987-8469

References

[1]. P.K. Pandey, S. Choubey, Y. Verma, M. Pandey, S.S.K. Kamal, K. Chandrashekhar, *Int. J. Environ. Res. Public Health*, **2007**, *4*, 332-339.

[2]. J. Cha, M. Cui, M. Jang, S.H. Cho, D.H. Moon, J. Khim, *Environ. Geochem. Health*, **2011**, *33*, 81–89.

[3]. Y.S. Ho, C.T. Huang, H.W. Huang, *Process Biochem.,* **2002**, *37*, 1421-1430.

[4]. Dupont, L., Bouanda, J., Dumoneau, J. and Applincourt M. *J. Colloid Interface Sci.,* **2003**, *263*, 35-41.

[5]. I. Villaescusa, M. Martinez, N. Miralles, *J. Chem. Technol. Biotechnol.,* **2000**, *74*, 812-816.

[6]. N. Feroze, M. Kazmi, W. Iqbal, S. Muhammad, *J. Environ. Protect. Ecology*, **2013**, *14*, 85-98.

[7]. E.F. Nassar, D. Zageer, M.S. Khlaf, *Orient. J. Phys. Sci.,* **2017,** *2*, 81-87.

[8]. C. Stötzel, F.A. Müeller, F. Reinert, F. Niederdraenk, J.E. Barralet, U. Gbureck, *Colloids Surf B Biointerfaces.,* **2009**, *74*, 91-95.

[9]. A.A. Alqadami, A.K. Moonis, O. Marta, R.S. Masoom, J. Byong-Hun, M. Khalid, *J. Clean. Product.,* **2018**, *178*,293-304.

[10]. S. Hassan, N.S. Awwad, A.H.A. Aboterika, *J. Hazard. Mater.,* **2008**, *154*, 992-7

[11]. B. Ramavandi, M. Shamsi, N. Abdolahi, *Pajouhan Scientific J*., **2014**, *12*, 58-64

[12]. M.S. Onyango, Y. Kojima, O. Aoyi, E.C. Bernardo, H. Matsuda, *J. Colloid Interface Sci*., **2004**, *279*, 341-350.

[13]. J.C. Elliot, *Structure and chemistry of the apatites and other calcium orthophosphates*, Elsevier Science B.V Netherlands, ***1994***, ISBN: 978-0-444-81582-1

[14]. K.H. Lim, T.T. Teng, M.H. Ibrahim, A. Ahmad, H.T. Chee, *APCBEE Proced.,* **2012**, *1*, 96–102.

[15]. N.S. Kumar, K. Min, *Chem. Eng. J.,* **2011**, *168*, 562-571.

[16]. S.K. Nadavala, K. Swayampakula, V.M. Boddu, K. Abburi, *J. hazard. Mater.,* **2009**, *162*,

482-489.
[17]. P.K. Pandey, Y. Verma, S. Choubey, M. Pandey, K. Chandrasekhar, *Bioresour. Technol*., **2007**, *99*, 4420-4427.
[18]. N. Abdel-Ghani, G. Fouad, E.M. Zahran, *Int. J. Environ. Sci. Technol*., **2015**, *12*, 211-222.
[19]. O. Keskinkan, M.Z.L. Goksu, M. Basibuyuk, C.F. Forster, *Bioresour. Technol.,* **2004**, *92*, 197-200.
[20]. M.M Rao, A. Ramesh, G.P. Rao, K. Seshaiah, *J. Hazard. Mater.,* **2006**, *129*, 123-129.
[21]. Q.S. Liu, T. Zheng, P. Wang, et al. *Chem. Eng. J.* **2010**, *157*, 348-356.
[22]. M.A.P. Cechinel, S.M.A.G.U. Souza, A.A.U. Souza, *J. Clean. Product.,* **2014**, *65*, 342-349
[23]. Y.S. HO, G. Mckay, *Process Biochem.*, **1999**, *34*, 451-465.
[24]. Weber Jr., W.J., Morris, J.C. and Sanit, J. *J. Sanit. Eng. Divis. Am. Soc. Civil Eng.*, **1963**, *89*, 31-38.
[25]. H. Aydın, B. Yasemin, Y. Cigdem, *J. Hazard. Mater.,* **2007**, *144*, 300-306.
[26]. P. Sivakumar, P.N. Palanisamy, *Indian J. Chem. Technol.,* **2011**, *18*, 188-196.
[27]. M.S. Venkata, N.C. Rao, J. Karthikeyan, *J. Hazard. Mater.*, **2002**, *90*, 189–204.

How to cite this manuscript: Mohamed N. Rashed*, Allia A. E. Gad, Nada M. Fathy, Adsorption of Cd (II) and Pb (II) Using Physically Pretreated Camel Bone Biochar, *Adv. J. Chem. A,* **2019**, 2(4), 347-364.